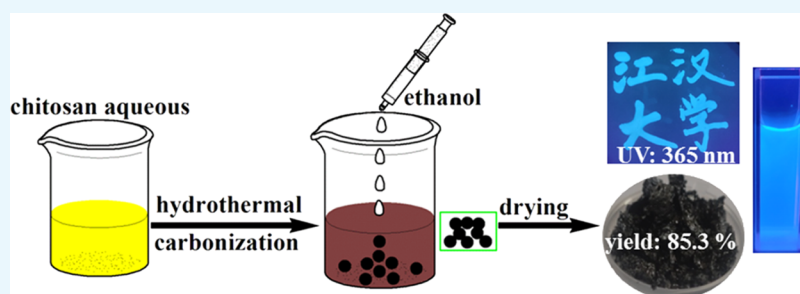


Ethanol-Precipitation-Assisted Highly Efficient Synthesis of Nitrogen-Doped Carbon Quantum Dots from Chitosan

Jun Zhan, Rujie Peng, Sixuan Wei, Jia Chen, Xianghong Peng,* and Biao Xiao*

Key Laboratory of Optoelectronic Chemical Materials and Devices of Ministry of Education, School of Chemistry and Environmental Engineering, Jiangnan University, Wuhan 430056, Hubei, China

Supporting Information



ABSTRACT: Nitrogen-doped carbon quantum dots (NCQDs) were prepared from chitosan through a hydrothermal reaction. When ethanol precipitation was used as the purification method, a high product yield of 85.3% was obtained. A strong blue fluorescence emission with a high quantum yield (QY) of 6.6% was observed from the NCQD aqueous solution. Physical and chemical characteristics of the NCQDs were carefully investigated by transmission electron microscopy (TEM), X-ray diffraction (XRD), Fourier transform infrared spectra (FTIR), Raman spectra, X-ray photoelectron spectroscopy (XPS), and transient fluorescence spectra. Experimental results showed that diameters of the NCQDs were in the range of 2–10 nm. The carbon quantum dots possess good water dispersibility and precipitation by ethanol. When used for metal ion detection, the detection limit of the NCQDs for Fe^{3+} was as low as $1.57 \mu\text{M}$. This work proposed a facile method to synthesize NCQDs from chitosan with high yield and demonstrated that carbon quantum dots derived from chitosan were promising for ion detection.

1. INTRODUCTION

Carbon quantum dots (CQDs) have received much attention due to their extraordinary properties, including excellent biocompatibility, low cytotoxicity, good cell permeability, and simple synthetic routes.^{1,2} As a new class of fluorescent carbon nanomaterials, CQDs have potential applications in multiple scientific fields, such as bioimaging, drug delivery, catalysts, energy conversion devices, optoelectronics, detection of metal ions, and so forth.^{3–6} Generally, synthetic routes of the CQDs could be classified into top-down and bottom-up approaches.⁷ The top-down methods refer to processes involving cutting larger carbon structures into smaller pieces, including chemical oxidation, electrochemical synthesis, arc-discharge and laser-ablation, and so on.² In these processes, the CQDs are formed from macroscopic carbon materials such as graphite, active carbon, graphene oxide, carbon nanotubes, coal, carbonized waste carbon paper, and biomass.^{7–9} By contrast, the bottom-up approaches refer to synthesize CQDs from organic molecular precursors using specific synthetic means such as microwave irradiation, hydrothermal treatments, ultra-sonication, and thermal combustion.⁷ To get high quality CQDs, usually, expensive starting materials, or high reaction temperature, or further complex surface-passivation is needed, hindering its large-scale commercialization. Therefore, explor-

ing simple, cheap and environmentally friendly way to synthesize CQDs is of great importance.

It is widely accepted that hydrothermal carbonization is a green, sustainable and facile method for synthesizing CQDs.^{2,7} Great efforts have been made to synthesize CQDs by hydrothermal method using biomass.^{10–14} These biomass-derived precursors are considered to be the most promising starting materials for CQDs because of its low cost, environmental friendliness, abundance and varieties of heteroatom doping.^{15–19} Chitosan is the second most abundant natural polymer that exists extensively in the shell of crustaceans. This kind of special macromolecule has significant applications in the biomaterial fields owing to its nontoxicity and biocompatibility.^{20,21} Previously, chitosan had been used to synthesize nitrogen-doped carbon dots (NCQDs) using the hydrothermal method under a mild reaction condition of 180°C .^{11,22} Zhang et al. reported an approach to synthesize NCQDs from chitosan by carbonization at 300°C , and quantum efficiency of the NCQDs was up to 4.34%.¹³ Nessim et al. proposed a method to synthesize NCQDs from chitosan using chemical vapor deposition, in which the obtained NCQDs exhibited a

Received: October 7, 2019

Accepted: December 6, 2019

Published: December 19, 2019

graphenelike structure.¹² As is known to all, post-treatments such as high-speed centrifugation, dialysis, and freeze drying are often adopted in the purification process. These operations are usually time-consuming and complicated.²³ To synthesize biomass-derived CQDs efficiently, it is important to simplify the purification process.

In this work, NCQDs were synthesized from chitosan by hydrothermal carbonization and purified via a simple ethanol precipitation process. The product yield of the NCQDs was as high as 85.3%, which was better than the previously reported scientific data on the yield of biomass-derived CQDs (Figure 1). Studies have shown that the NCQDs had a strong blue

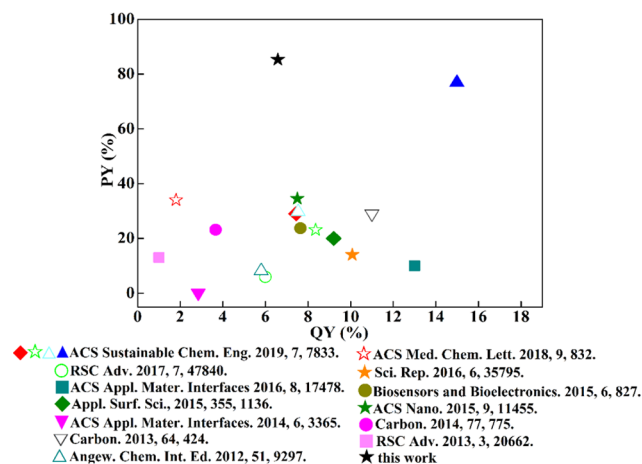


Figure 1. Statistical product yields vs quantum yield of the recently reported biomass-derived CQDs from the science database.

fluorescence emission with a high quantum yield (QY) of 6.6%, and the NCQDs exhibited excellent metal ion detection ability. This work might benefit for the applications of NCQDs on a large scale.

2. RESULTS AND DISCUSSION

2.1. Morphology and Chemical Composition. The morphology of the NCQDs is shown in Figure 2a. Clearly, the

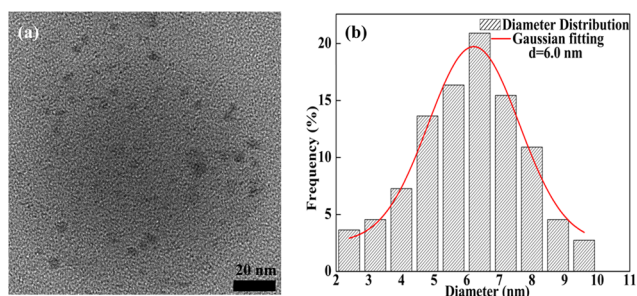


Figure 2. (a) HRTEM image of the NCQDs. (b) Statistical diameter distribution of the NCQDs from HRTEM images.

synthesized NCQDs were uniform in size and had a nearly spherical shape. The NCQDs had a narrow size distribution, and its diameters were in the range of 2–10 nm. The gaussian fitting curve (based on more than 100 particles) showed that the average size of the NCQDs was 6 nm, as shown in Figure 2b.

XRD patterns of the chitosan and the NCQDs are presented in Figure 3a. The chitosan sample showed diffraction peaks at

$2\theta = 20^\circ$ and 11° , which were deemed as the characteristic crystallization peak and the amorphous peak, respectively.¹³ After hydrothermal carbonization, the crystalline peak of chitosan had diminished and a new peak at $2\theta = 25^\circ$ with a large full width at half maximum (FWHM) was observed. Disappearance of the characteristic crystalline peaks and appearance of a broad new diffraction peak revealed that chitosan had been completely carbonized and an amorphous carbon phase was formed.¹⁷

FTIR spectra of the chitosan and the NCQDs are shown in Figure 3b. For the NCQDs, absorptions at $3500\text{--}3200$, $1695\text{--}1570$, and 1400 cm^{-1} were strengthened, indicating the existence of O–H/N–H, C=O, and N–H bands (attributed to amide groups) and COOH bands, respectively. Incidentally, these polar units were responsible for the good dispersity of the NCQDs in water. For the chitosan, the C–H stretching bands obviously disappeared or weakened at 2880 and $1130\text{--}1064\text{ cm}^{-1}$, illustrating the depolymerization of the chitosan chains and the decomposition of the pyranose rings during carbonization. The presence of C=O bands demonstrated that carboxyl or carbonyl moieties existed in the NCQDs, which was consistent with the XPS results.^{11,17}

The Raman spectrum of the NCQDs showed a disordered (D) band at 1350 cm^{-1} and a crystalline (G) band at 1585 cm^{-1} (Figure 3c). The D band is generally due to amorphous sp^3 carbon, and the G band belongs to the crystalline sp^2 carbon of graphitic domains and the in-plane vibration of sp^2 carbon-bonded atoms.^{24,25} The intensity ratio of D to G bands (I_D/I_G ratio) was 0.87, which indicated partially the existence of disorientation and stacking of graphene sheets in NCQDs.²⁴

Further information on the composition of the NCQDs was obtained by X-ray photoelectron spectroscopy (XPS) as shown in Figure 4a. The survey scan performed in the $0\text{--}1350\text{ eV}$ binding energy range showed characteristic peaks of elements C, O, and N. The integral area ratio of C/O/N was about 9:4:1. By careful analysis of the C 1s peaks between 281 and 291 eV (Figure 4b), four peaks at 284.60, 285.40, 286.10, and 288.37 eV were found, which should be attributed to the C–C/C=C, C–N, C–O, and C=O bonds, respectively.²⁶ It should be noted that the characteristic peak at around 284.60 eV was an indication of sp^2 aromatic or graphitic structures.¹⁷ The appearance of C–O and C=O signals could confirm the existence of carbonyl and carboxyl groups in NCQDs.¹⁷ Moreover, the N 1s spectrum of the NCQDs (Figure 4c) showed predominant peaks at 399.80 and 400.60 eV, which were caused by the N–H and C=N interactions.^{13,27} The O 1s spectrum (Figure 4d) presented two peaks at 532.01 and 533.17 eV, which were attributed to C=O and C–O bonds, respectively.¹³ The XPS results suggested that there existed hydrophilic functional groups on the surface of the NCQDs. The hydrophilic property of the NCQDs could be further confirmed by the surface potential measurement, as shown in Figure S1.

According to the discussions above, the possible reaction route for the synthesis of the NCQDs was as follows: the interactions between the positive charges in the protonated amino groups of chitosan and the negative charges in the carboxylate groups of citric acid lead to the formation of a chitosan–citrate complex.²⁸ Such a complex first forms a polymerlike structure and then is further carbonized to form NCQDs with carboxyl, hydroxyl, and amino groups on its surface. This synthetic mechanism (Figure 5) was similar to that in a previous report.²⁹ It should be emphasized that the

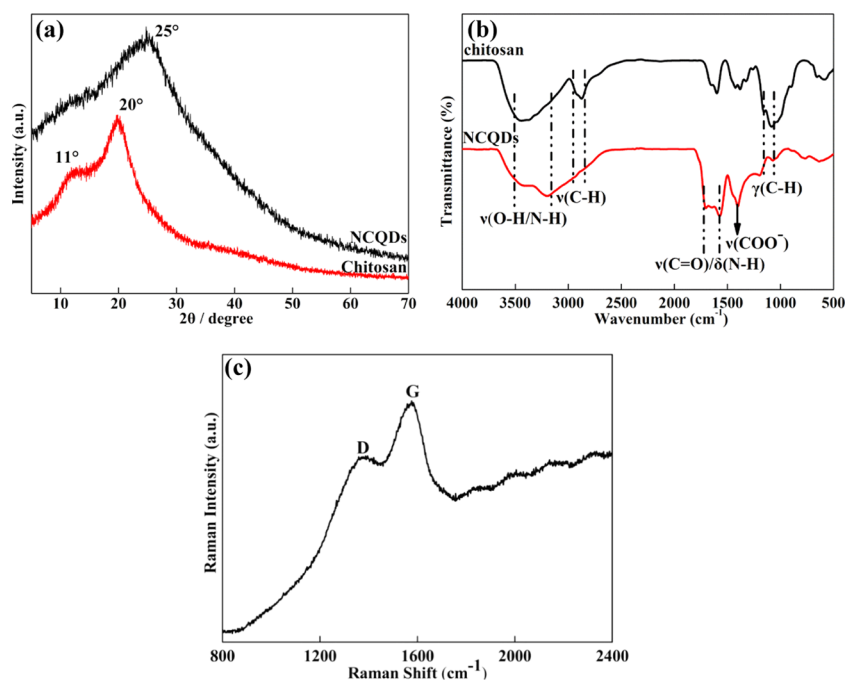


Figure 3. (a) XRD patterns of the NCQDs and chitosan. (b) Fourier transform infrared spectra (FTIR) spectra of chitosan and NCQDs. (c) Raman spectra of the NCQDs.

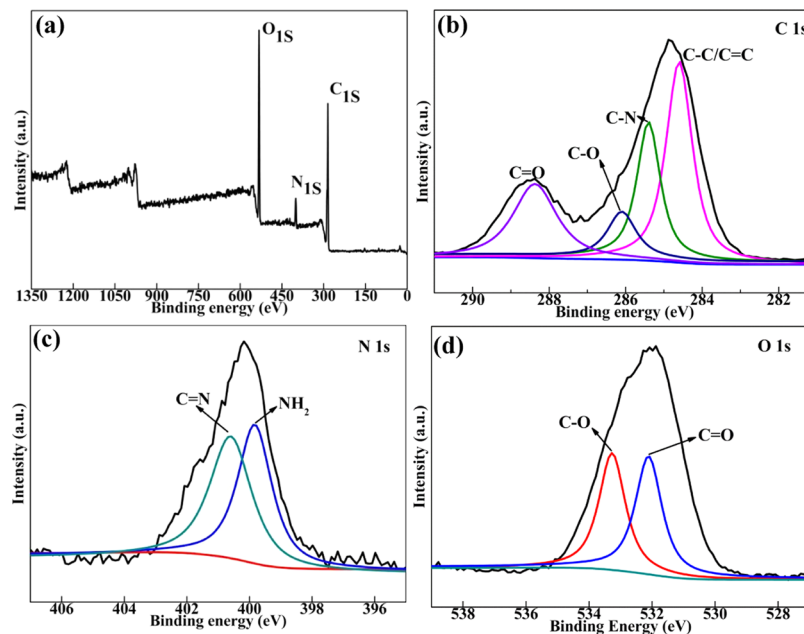


Figure 4. (a) Full scan of the XPS spectra, (b) C 1s XPS spectra, (c) N 1s XPS spectra, and (d) O 1s XPS spectra of as-prepared NCQDs.

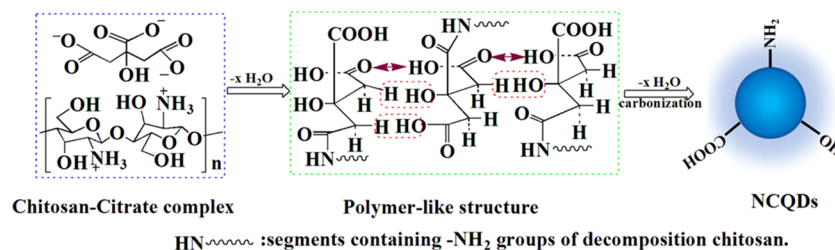


Figure 5. Possible reaction route for the synthesis of the NCQDs.

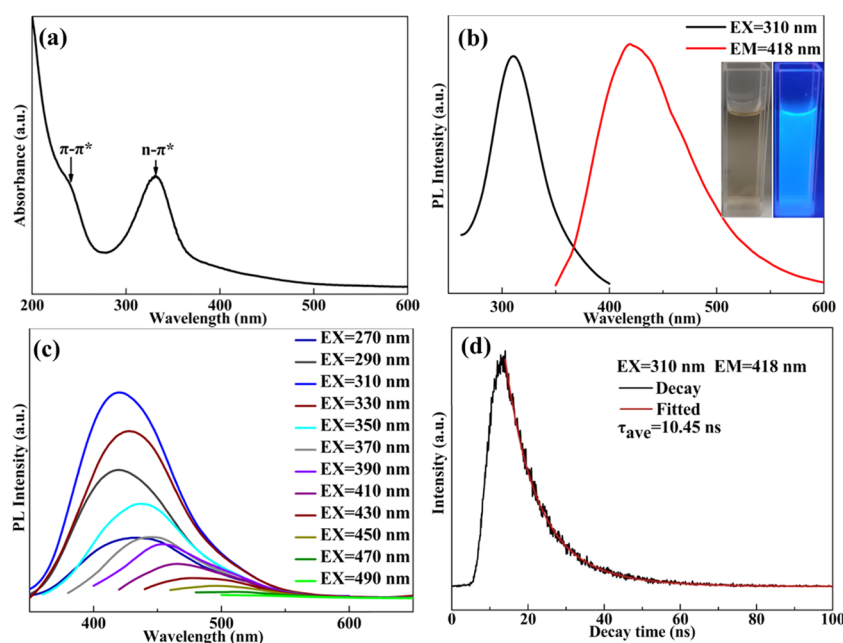


Figure 6. (a) UV–vis absorption spectra. (b) fluorescence excitation (black line, $\lambda_{\text{ex}} = 310$ nm) and emission spectra (red line, $\lambda_{\text{em}} = 418$ nm) of the NCQDs dispersed in water at room temperature. (inset: photograph of chitosan NCQDs under daylight and UV radiation). (c) Fluorescence emission spectra of the NCQDs obtained at different excitation wavelengths with a 20 nm increment from 270 to 490 nm. (d) Time-resolved PL decay and fitting curves for the as-prepared NCQDs.

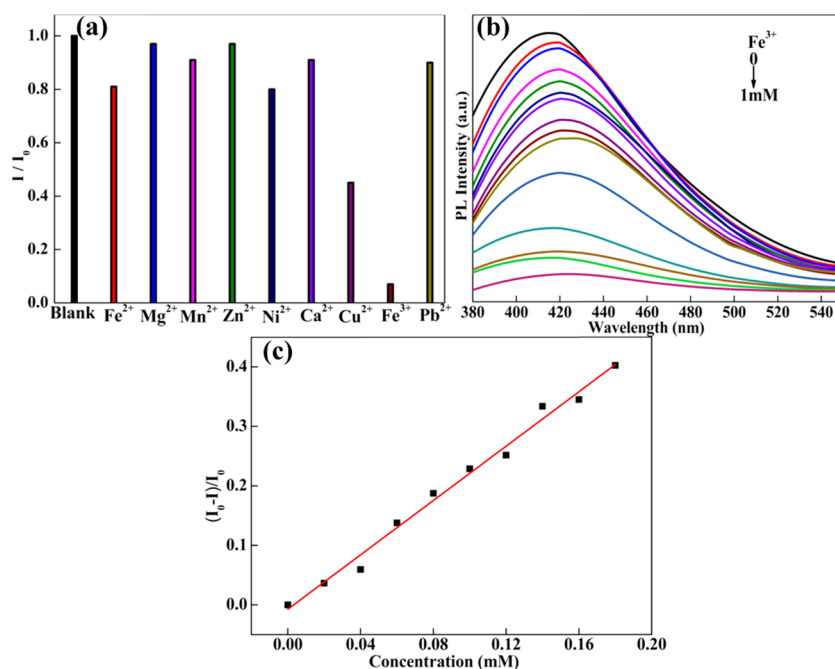


Figure 7. Fluorescence response of NCQDs by metal ions: (a) Fluorescence quenching induced by different metal ions at a concentration of 1 mM (I_0 and I are the fluorescence intensities of the NCQD aqueous dispersion without and with metal ions, respectively). (b) Fluorescence spectra of NCQDs at various concentrations of Fe^{3+} ranging from 0 to 1 mM. The excitation wavelength is fixed at 310 nm. (c) Linear relationship between fluorescence and Fe^{3+} concentration at 0–0.18 mM.

NCQD powder could be well dispersed in aqueous solutions (>40 mg/mL). When ethanol was added to the NCQD solution, the intermolecular hydrogen bond between NCQDs and water was destroyed, and the $-\text{COOH}$ and $-\text{NH}_2$ groups on its surface formed a strong hydrogen bond. These features were beneficial for the precipitation and purification of the NCQDs, leading to the final high product yield of 85.3%. It should be noted that such a productivity was much higher than

those CQDs obtained from the traditional hydrothermal method (see Figure 1).

2.2. Optical Properties of CQDs. UV–vis absorption of the NCQDs (Figure 6a) showed an absorption peak at 330 nm with a shoulder at around 240 nm, which were aroused from $\pi-\pi^*$ transition of the $\text{C}=\text{C}$ bonds and $n-\pi^*$ transition of the $\text{C}=\text{O}$ bonds.³⁰ As shown in Figure 6b, the NCQDs displayed a maximum emission at 418 nm when excited with a 310 nm

light. The FWHM was 108 nm, indicating a complex fluorescence emission from the NCQDs.²⁹ The aqueous solution of the NCQDs showed strong blue light emission under UV irradiation. When exposed to the daylight, the solution changed back to translucent yellow (right inset, Figure 6b). As shown in Figure 6c, the NCQDs exhibited typical excitation-dependent photoluminescent behavior, which was similar to previous reports.^{31,32} Upon increasing the excitation wavelength from 270 to 490 nm, the emission peak red-shifted from 418 to 530 nm. Such behavior could be explained by the broad distribution of different emissive sites in the NCQDs.³¹

In consideration of its strong luminous property, the NCQD aqueous solution (20 mg/mL) was utilized as ink for writing. The Chinese characters “江汉大学” written from the ink emitted a strong fluorescence when excited with UV lamps, as shown in Figure S2. When mixed with poly(vinyl alcohol) (PVA) solution, the NCQDs/PVA composite film precursor was obtained. Figure S3 shows the fluorescence microscopy images of the PVA/NCQD film with daylight, UV, blue, and green light excitation. The multicolor emission effect of the composite film suggested that the NCQDs were promising for electronic labels and biological imaging.

The maximum photoluminescence (PL) quantum yield was measured to be 6.6% when at 418 nm blue fluorescence was emitted. The average lifetime of the NCQDs was fitted to be 10.45 ns, as shown in Figure 6d. The lifetime of the NCQDs was longer than the previously reported values, suggesting that the NCQDs in this work were suitable for optoelectronic and biological applications.³³

2.3. Detection of Metal Ions. Metal ions are widely distributed in the environmental and biological systems.³⁴ Accurate detection of the metal ion content is of significant importance for the ecosystems and life systems.^{33,35} Different from other methods, the fluorescence detection method has unique advantages such as high sensitivity, simple operation, convenient monitoring, and fast reaction.³³ To evaluate the selectivity of the NCQDs for metal ion detection, different metal ions, including Mg^{2+} , Mn^{2+} , Fe^{2+} , Zn^{2+} , Co^{2+} , Ni^{2+} , Cu^{2+} , Fe^{3+} , and Pb^{2+} , were used as target ions. Detection results are shown in Figure 7a. Through analysis of the fluorescence intensity ratio I/I_0 (where I and I_0 are the fluorescence intensities at 418 nm after and before the addition of target ions), it was found that the NCQDs had a universal detecting ability for many ions. Specifically, the fluorescence intensity ratio for Fe^{3+} detection was the lowest with a value of 0.1, demonstrating the high detectivity of the NCQDs for Fe^{3+} .

To further study the Fe^{3+} sensitivity of the NCQDs, Fe^{3+} ions with different concentrations were added into the NCQDs aqueous solution and the fluorescence intensities were measured. As shown in Figure 7b, the PL intensities decreased with the increase of Fe^{3+} concentration. This was easy to understand since the chelation between Fe^{3+} ions and phenolic hydroxy groups could reduce fluorescence emission from the NCQDs.⁸ Figure 7c depicts the relationship of the fluorescence quenching value $\Delta I/I_0$ with the concentration of Fe^{3+} , where $\Delta I = I_0 - I$. Obviously, the fluorescence quenching values presented an almost linear relationship in the range of 0–0.18 mM. The theoretical lower detection limit was calculated to be $1.57 \mu\text{M}$ ($= 3\sigma/m$, where σ is the standard deviation and m is the slope of the linear response region), which was much lower than most of the previously reported values as shown in Table 1. The results clearly suggested that

the NCQDs in this contribution had high sensitivity in metal ion detection.

Table 1. Comparison of the Detection Limit of Fe^{3+} by Different Sensing Systems

fluorescent probes	detection limit (μM)	refs
pyrazoline derivative	1.4	4
rhodamine-based RPE	5	5
phosphazene	4.8	36
GO nanosheets	17.9	8
GQD-BMIM	7.22	37
N-GQDs	0.09	38
S-GQDs	0.0042	33
N-CQDs	1.57	this work

3. CONCLUSIONS

We have successfully synthesized NCQDs from chitosan. A simple ethanol precipitation procedure was adopted for purification. The product yield of the NCQDs was as high as 85.3%. The synthesized NCQDs possessed excellent water dispersity ($>40 \text{ mg/mL}$) due to the hydrophilic functional groups on the surface. Spectral studies had shown that the NCQDs could reach a high quantum yield of 6.6%. The metal ion detection experiment illustrated that the NCQDs have universal ion detection capability and is especially suitable for Fe^{3+} monitoring. This contribution may be beneficial for the large-scale production and application of NCQDs.

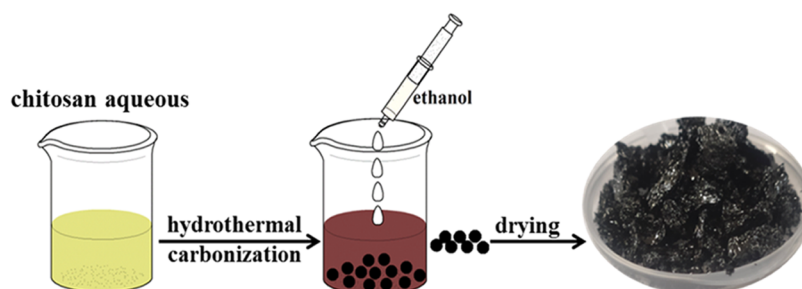
4. EXPERIMENTAL SECTION

4.1. Materials. Chitosan powder (DD $\geq 95\%$, 100–200 mPa s) and lead(II) acetate trihydrate (A.R.) were purchased from Macklin Reagent Biochemical Co. Ltd. The other reagents were purchased from Shanghai Sinopharm Reagent Co. All reagents were of analytical grade and used without further purification.

4.2. Synthesis of CQDs. Chitosan powder was dissolved in 0.5 M citric acid (CA) solution to obtain 1 wt % chitosan aqueous solution. The chitosan aqueous solution and urea were added to a 25 mL Teflon container that was packed into a stainless steel autoclave. Then, the experimental installation was heated to 180°C and kept for 10 h. After that, the autoclave was cooled to room temperature in the air. The obtained aqueous solution was first mixed with CH_2Cl_2 , and then, the underlying aqueous solution was removed. Afterward, the aqueous solution was filtered with a $0.22 \mu\text{m}$ filter membrane and ethanol was employed for precipitation. The precipitate was centrifuged (3600 rpm), and the final product was dried at 60°C for 6 h. The obtained solid powder was denoted CQDs. The details of the synthesis of NCQDs is illustrated in Scheme 1.

4.3. Characterization. The morphology of the NCQDs was characterized by transmission electron microscopy (TEM; HT7700 EXALENS, operated at 200 kV). The size distribution of the NCQDs was calculated based on their TEM images. X-ray diffraction (XRD) patterns were carried on an XRD diffractometer (D8 Advance, Bruker, PANalytical) with $\text{Cu K}\alpha$ radiation ($\lambda = 0.15406 \text{ nm}$). Raman spectroscopy (Renishaw, 532 nm laser) was employed to characterize the structure of the samples. X-ray photoelectron spectroscopy (XPS) measurements were performed on a Thermo ESCALAB 250XI X-ray spectrometer (Thermo Scientific) with mono-

Scheme 1. Synthesis of NCQDs from the Hydrothermal Treatment of Chitosan Aqueous Solution



chromatic Al K α (1486.7 eV). The samples were recorded on a TENSOR 27 FTIR spectrometer (Bruker, Germany) with KBr powder as the background, ranging from 4000 to 500 cm^{-1} . The ζ -potential was measured on a Malvern Nano ZS instrument (Malvern). Optical absorption was measured on a UV-2550 (Shimadzu, Japan) spectrometer. Fluorescence spectra were recorded on an LS-55 fluorescence spectrometer (PE) with a slit width of 5 nm for excitation and emission. The excitation was increased by a 20 nm increment starting from 270 to 490 nm. All of the optical spectra were recorded with a quartz cuvette of 1 cm path length. Fluorescence decay curves and photoluminescence (PL) quantum yield (QY) of the as-prepared NCQDs were measured at room temperature using an Edinburgh FLSP 920 spectrometer (Edinburgh Instruments) equipped with an integrating sphere under 310 nm excitation.

4.4. Detection of Metal Ions. Different concentrations of Fe^{3+} aqueous solutions (0–0.20 mM, interval of 0.02 mM; 0.20–1.0 mM, interval of 0.2 mM) and other metal ion solutions (1.0 mM) were freshly prepared. To evaluate the sensitivity of the NCQDs to Fe^{3+} , the Fe^{3+} solutions of different concentrations were mixed with 0.01 mg/mL NCQD aqueous dispersion at 1:1 volume ratio. After 5 min of equilibration, fluorescence from the mixed solutions was detected by a fluorescence spectrophotometer. Other metal ionic solutions were mixed and detected with the NCQDs in the same way. All of the experiments were performed at room temperature.

■ ASSOCIATED CONTENT

Supporting Information

The Supporting Information is available free of charge at <https://pubs.acs.org/doi/10.1021/acsomega.9b03318>.

Surface charge profile of NCQDs obtained by a Malvern Nano instrument (Figure S1), NCQD ink (20 mg/mL) gave fluorescence words under a UV lamp at 365 and 254 nm (Figure S2), fluorescence microscopy images of PVA/NCQD film with (a) daylight, (b) UV, (c) blue, and (d) green light excitation (Figure S3) (PDF)

■ AUTHOR INFORMATION

Corresponding Authors

*E-mail: pxh@jhun.edu.cn (X.P.).

*E-mail: biaoxiao@jhun.edu.cn (B.X.).

ORCID

Biao Xiao: 0000-0003-4969-0842

Notes

The authors declare no competing financial interest.

■ ACKNOWLEDGMENTS

This work was financially supported by the National Natural Science Foundation of China (51703081), the Hubei Natural Science Foundation (2019CFB198), the Guiding Project of Education Department of Hubei Province (B2018259), the Discipline Cultivation Plan of Material Science and Engineering, Jiangnan University (03100023).

■ REFERENCES

- (1) Wang, W.; Wang, Z.; Liu, J.; Peng, Y.; Yu, X.; Wang, W.; Zhang, Z.; Sun, L. One-pot facile synthesis of graphene quantum dots from rice husks for Fe^{3+} sensing. *Ind. Eng. Chem. Res.* **2018**, *57*, 9144.
- (2) Bhandari, S.; Monda, D.; Nataraj, S. K.; Balakrishna, R. G. Biomolecule-derived quantum dots for sustainable optoelectronics. *Nanoscale Adv.* **2019**, *1*, 913.
- (3) Xie, C.; Fan, T.; Wang, A.; Chen, S. Enhanced visible-light photocatalytic activity of a TiO_2 membrane-assisted with N-doped carbon quantum dots and SiO_2 opal photonic crystal. *Ind. Eng. Chem. Res.* **2019**, *58*, 120.
- (4) Hu, S.; Zhang, S.; Gao, C.; Xu, C.; Gao, Q. A new selective fluorescent sensor for Fe^{3+} based on a pyrazoline derivative. *Spectrochim. Acta, Part A* **2013**, *113*, 325.
- (5) Wei, Y.; Aydin, Z.; Zhang, Y.; Liu, Z.; Guo, M. A turn-on fluorescent sensor for imaging labile Fe^{3+} in live neuronal cells at subcellular resolution. *ChemBioChem* **2012**, *13*, 1569.
- (6) Wang, Y.; Wang, K.; Han, Z.; Yin, Z.; Zhou, C.; Du, F.; Zhou, S.; Chen, P.; Xie, Z. High color rendering index trichromatic white and red LEDs prepared from silane-functionalized carbon dots. *J. Mater. Chem. C* **2017**, *5*, 9629.
- (7) Wang, R.; Lu, K.; Tang, Z.; Xu, Y. Recent progress in carbon quantum dots: synthesis, properties and applications in photocatalysis. *J. Mater. Chem. A* **2017**, *5*, 3717.
- (8) Wang, D.; Wang, L.; Dong, X.; Shi, Z.; Jin, J. Chemically tailoring graphene oxides into fluorescent nanosheets for Fe^{3+} ion detection. *Carbon* **2012**, *50*, 2147.
- (9) Yuan, F.; Li, S.; Fan, Z.; Meng, X.; Fan, L.; Yang, S. Shining carbon dots: synthesis and biomedical and optoelectronic applications. *Nano Today* **2016**, *11*, 565.
- (10) Liang, Q.; Ma, W.; Shi, Y.; Li, Z.; Yang, X. Easy synthesis of highly fluorescent carbon quantum dots from gelatin and their luminescent properties and applications. *Carbon* **2013**, *60*, 421.
- (11) Yang, Y.; Cui, J.; Zheng, M.; Hu, C.; Tan, S.; Xiao, Y.; Yang, Q.; Liu, Y. One-step synthesis of amino-functionalized fluorescent carbon nanoparticles by hydrothermal carbonization of chitosan. *Chem. Commun.* **2012**, *48*, 380.
- (12) Kumar, S.; Aziz, S. T.; Girshevitz, O.; Nessim, G. D. One-step synthesis of N-doped graphene quantum dots from chitosan as a sole precursor using chemical vapor deposition. *J. Phys. Chem. C* **2018**, *122*, 2343.
- (13) Liu, X.; Pang, J.; Xu, F.; Zhang, X. Simple approach to synthesize amino-functionalized carbon dots by carbonization of chitosan. *Sci. Rep.* **2016**, *6*, No. 31100.

- (14) Liu, M. L.; Chen, B. B.; Li, C. M.; Huang, C. Z. Carbon dots: synthesis, formation mechanism, fluorescence origin and sensing applications. *Green Chem.* **2019**, *21*, 449.
- (15) Zhao, S.; Lan, M.; Zhu, X.; Xue, H.; Ng, T. W.; Meng, X.; Lee, C. S.; Wang, P.; Zhang, W. Green synthesis of bifunctional fluorescent carbon dots from garlic for cellular imaging and free radical scavenging. *ACS Appl. Mater. Interfaces* **2015**, *7*, 17054.
- (16) Zhang, M.; Wang, W.; Yuan, P.; Chi, C.; Zhang, J.; Zhou, N. Synthesis of lanthanum doped carbon dots for detection of mercury ion, multi-color imaging of cells and tissue, and bacteriostasis. *Chem. Eng. J.* **2017**, *330*, 1137.
- (17) Liang, Z.; Zeng, L.; Cao, X.; Wang, Q.; Wang, X.; Sun, R. Sustainable carbon quantum dots from forestry and agricultural biomass with amplified photoluminescence by simple NH_4OH passivation. *J. Mater. Chem. C* **2014**, *2*, 9760.
- (18) Yang, S.; Sun, J.; Li, X.; Zhou, W.; Wang, Z.; He, P.; Ding, G.; Xie, X.; Kang, Z.; Jiang, M. Large-scale fabrication of heavy doped carbon quantum dots with tunable-photoluminescence and sensitive fluorescence detection. *J. Mater. Chem. A* **2014**, *2*, No. 8660.
- (19) Qu, D.; Zheng, M.; Du, P.; Zhou, Y.; Zhang, L.; Li, D.; Tan, H.; Zhao, Z.; Xie, Z.; Sun, Z. Highly luminescent S, N co-doped graphene quantum dots with broad visible absorption bands for visible light photocatalysts. *Nanoscale* **2013**, *5*, 12272.
- (20) Fang, Y.; Zhang, R.; Duan, B.; Liu, M.; Lu, A.; Zhang, L. Recyclable universal solvents for chitin to chitosan with various degrees of acetylation and construction of robust hydrogels. *ACS Sustainable Chem. Eng.* **2017**, *5*, 2725.
- (21) Zhu, K.; Duan, J.; Guo, J.; Wu, S.; Lu, A.; Zhang, L. High-strength films consisted of oriented chitosan nanofibers for guiding cell growth. *Biomacromolecules* **2017**, *18*, 3904.
- (22) Zhao, L.; Baccile, N.; Gross, S.; Zhang, Y.; Wei, W.; Sun, Y.; Antonietti, M.; Titirici, M. Sustainable nitrogen-doped carbonaceous materials from biomass derivatives. *Carbon* **2010**, *48*, 3778.
- (23) Zhang, X.; Jiang, M.; Niu, N.; Chen, Z.; Li, S.; Liu, S.; Li, J. Natural-product-derived carbon dots: from natural products to functional materials. *ChemSusChem* **2018**, *11*, 11.
- (24) Sefidan, S. B.; Eskandari, H.; Shamkhali, A. N. Rapid colorimetric flow injection sensing of hypochlorite by functionalized graphene quantum dots. *Sens. Actuators, B* **2018**, *275*, 339.
- (25) Li, Y.; Zhao, Y.; Cheng, H.; Hu, Y.; Shi, G.; Dai, L.; Qu, L. Nitrogen-doped graphene quantum dots with oxygen-rich functional groups. *J. Am. Chem. Soc.* **2012**, *134*, 15.
- (26) Wang, G.; Guo, Q.; Chen, D.; Liu, Z.; Zheng, X.; Xu, A.; Yang, S.; Ding, G. Facile and highly effective synthesis of controllable lattice sulfur-doped graphene quantum dots via hydrothermal treatment of durian. *ACS Appl. Mater. Interfaces* **2018**, *10*, 5750.
- (27) Liu, X.; Jiang, H.; Ye, J.; Zhao, C.; Gao, S.; Wu, C.; Li, C.; Li, J.; Wang, X. Nitrogen-doped carbon quantum dot stabilized magnetic iron oxide nanoprobe for fluorescence, magnetic resonance, and computed tomography triple-modal in vivo bioimaging. *Adv. Funct. Mater.* **2016**, *26*, 8694.
- (28) Watthanaphanit, A.; Supaphol, P.; Furuike, T.; Tokura, S.; Tamura, H.; Rujiravanit, R. Novel chitosan-spotted alginate fibers from wet-spinning of alginate solutions containing emulsified chitosan-citrate complex and their characterization. *Biomacromolecules* **2009**, *10*, 320.
- (29) Zhu, S.; Meng, Q.; Wang, L.; Zhang, J.; Song, Y.; Jin, H.; Zhang, K.; Sun, H.; Wang, H.; Yang, B. Highly photoluminescent carbon dots for multicolor patterning, sensors, and bioimaging. *Angew. Chem., Int. Ed.* **2013**, *52*, 3953.
- (30) Pan, D.; Zhang, J.; Li, Z.; Wu, M. Hydrothermal route for cutting graphene sheets into blue-luminescent graphene quantum dots. *Adv. Mater.* **2010**, *22*, 734.
- (31) Sun, Y.; Zhou, B.; Lin, Y.; Wang, W.; Fernando, K. A. S.; Pathak, P.; Mezziani, M. J.; Harruff, B. A.; Wang, X.; Wang, H.; Luo, P. G.; Yang, H.; Kose, M. E.; Chen, B.; Veca, L. M.; Xie, S. Quantum-sized carbon dots for bright and colorful photoluminescence. *J. Am. Chem. Soc.* **2006**, *128*, 7756.
- (32) Zheng, M.; Liu, S.; Li, J.; Qu, D.; Zhao, H.; Guan, X.; Hu, X.; Xie, Z.; Jing, X.; Sun, Z. Integrating oxaliplatin with highly luminescent carbon dots: an unprecedented theranostic agent for personalized medicine. *Adv. Mater.* **2014**, *26*, 3554.
- (33) Wang, L.; Zhou, H. S. Green synthesis of luminescent nitrogen-doped carbon dots from milk and its imaging application. *Anal. Chem.* **2014**, *86*, 8902.
- (34) Luo, X.; Lei, X.; Cai, N.; Xie, X.; Xue, Y.; Yu, F. Removal of heavy metal ions from water by magnetic cellulose-based beads with embedded chemically modified magnetite nanoparticles and activated carbon. *ACS Sustainable Chem. Eng.* **2016**, *4*, 3960.
- (35) Zheng, M.; Tan, H.; Xie, Z.; Zhang, L.; Jing, X.; Sun, Z. Fast response and high sensitivity europium metal organic framework fluorescent probe with chelating terpyridine sites for Fe^{3+} . *ACS Appl. Mater. Interfaces* **2013**, *5*, 1078.
- (36) Kagit, R.; Yildirim, M.; Ozay, O.; Yesilot, S.; Ozay, H. Phosphazene based multicentered naked-eye fluorescent sensor with high selectivity for Fe^{3+} ions. *Inorg. Chem.* **2014**, *53*, 2144.
- (37) Ananthanarayanan, A.; Wang, X.; Routh, P.; Sana, B.; Lim, S.; Kim, D.; Lim, K.; Li, J.; Chen, P. Facile synthesis of graphene quantum dots from 3D graphene and their application for Fe^{3+} Sensing. *Adv. Funct. Mater.* **2014**, *24*, 3021.
- (38) Ju, J.; Chen, W. Synthesis of highly fluorescent nitrogen-doped graphene quantum dots for sensitive, label-free detection of Fe (III) in aqueous media. *Biosens. Bioelectron.* **2014**, *58*, 219.